Assessing Induced Folding of an Intrinsically Disordered Protein by Site-Directed Spin-Labeling Electron Paramagnetic Resonance Spectroscopy

Benjamin Morin,[†,‡] Jean-Marie Bourhis,[†,‡] Valérie Belle,[§] Mireille Woudstra,[§] Frédéric Carrière,[||] Bruno Guigliarelli,[§] André Fournel,[*,§] and Sonia Longhi[*,‡]

Architecture et Fonction des Macromolécules Biologiques, UMR 6098 CNRS et Universités Aix-Marseille I et II, Campus de Luminy, 163 Avenue de Luminy, Case 932, 13288 Marseille Cedex 09, France, Bioénergétique et Ingénierie des Protéines, UPR 9036 CNRS, 31 Chemin Joseph Aiguier, 13402 Marseille Cedex, France, Université Aix-Marseille I, 3 Place Victor Hugo, 13331 Marseille Cedex 3, France, and Enzymologie Interfaciale et Physiologie de la Lipolyse, UPR 9025, 31 Chemin Joseph Aiguier, 13402 Marseille Cedex, France

Received: June 14, 2006; In Final Form: August 2, 2006

We used site-directed spin-labeling electron paramagnetic resonance (EPR) spectroscopy to study the induced folding of the intrinsically disordered C-terminal domain of measles virus nucleoprotein (N_{TAIL}). Four single-site N_{TAIL} mutants (S407C, S488C, L496C, and V517C), located in three conserved regions, were prepared and labeled with a nitroxide paramagnetic probe. We could monitor the gain of rigidity that N_{TAIL} undergoes in the presence of either the secondary structure stabilizer 2,2,2-trifluoroethanol (TFE) or one of its physiological partners, namely, the C-terminal domain (XD) of the viral phosphoprotein. The mobility of the spin label grafted at positions 488, 496, and 517 was significantly reduced upon addition of XD, contrary to that of the spin label bound to position 407, which was unaffected. Furthermore, the EPR spectra of spin-labeled S488C and L496C bound to XD in the presence of 30% sucrose are indicative of the formation of an α-helix in the proximity of the spin labels. Such an α-helix had been already identified by previous biochemical and structural studies. Using TFE we unveiled a previously undetected structural propensity within the N-terminal region of N_{TAIL} and showed that its C-terminal region "resists" gaining structure even at high TFE concentrations. Finally, we for the first time showed the reversibility of the induced folding process that N_{TAIL} undergoes in the presence of XD. These results highlight the suitability of site-directed spin-labeling EPR spectroscopy to identify protein regions involved in binding and folding events, while providing insights at the residue level.

Introduction

Intrinsically disordered proteins (IDPs) are functional proteins that fulfill essential biological functions while lacking highly populated and uniform secondary and tertiary structures under physiological conditions.[1−7] IDPs show an extremely wide diversity in their structural properties. Indeed they can attain extended conformations (random-coil-like) or remain globally collapsed (molten-globule-like), where the latter possess regions of fluctuating secondary structure.[8] Conformational and spectroscopic analyses showed that random-coil-like proteins can be subdivided in their turn into two major groups. While the first group consists of proteins with extended maximum dimensions typical of random coils with no (or little) secondary structure, the second group comprises the so-called premolten globules, which are more compact (but still less compact than globular or molten globule proteins) and conserve some residual secondary structure.[1,3] It has been proposed that the residual intramolecular interactions that typify the premolten globule state may enable a more efficient start of the folding process induced by a partner.[2,9−11]

Measles virus (MV) is an enveloped RNA virus within the *Morbillivirus* genus of the Paramyxoviridae family. Its non-segmented, negative-sense, single-stranded RNA genome is encapsidated by the viral nucleoprotein (N) within a helical nucleocapsid. Transcription and replication are carried out onto this N/RNA complex by the viral polymerase complex which consists of two components, the large protein (L) and the phosphoprotein (P) (reviewed in ref 12).

MV nucleoprotein is divided into two regions: a structured N-terminal moiety, N_{CORE} (aa 1−400), which contains all the regions necessary for self-assembly and RNA-binding,[13,14] and a C-terminal domain, N_{TAIL} (aa 401−525) that is intrinsically unstructured[15] and is exposed at the surface of the viral nucleocapsid.[13,16,17] Thanks to its intrinsic flexible nature, N_{TAIL} interacts with various partners, including host cell proteins[18−24] and the P protein.[14,15] The P protein is an essential subunit of the viral polymerase complex in that it tethers the L protein onto the nucleocapsid template. P is a modular protein,[25,26] whose C-terminal X domain (XD, aa 459−507 of P) is responsible for binding to N_{TAIL}.[14,27] We have previously reported the crystal structure of XD[27] and shown that XD induces α-helical folding of N_{TAIL}.[27] Within a conserved region of N_{TAIL} (aa 489−506, Box2), an α-helical molecular recognition element (α-MoRE),[28] involved in binding to P and induced folding was identified (aa 489−499)[27,29] and then observed in

* Authors to whom correspondence should be addressed. Phone: (33) 4 91 16 45 57 (A.F.); (33) 4 91 82 55 80 (S.L.). Fax: (33) 4 91 16 45 78 (A.F.); (33) 4 91 26 67 20 (S.L.). E-mail: Fournel@ibsm.cnrs-mrs.fr; Sonia.Longhi@afmb.univ-mrs.fr.

† These authors contributed equally to this work

‡ Architecture et Fonction des Macromolécules Biologiques, UMR 6098 CNRS, and Universités Aix-Marseille I et II.

§ Bioénergétique et Ingénierie des Protéines, UPR 9036 CNRS, and Université Aix-Marseille I.

|| Enzymologie Interfaciale et Physiologie de la Lipolyse, UPR 9025.

10.1021/jp063708u CCC: $33.50
Published on Web 09/20/2006

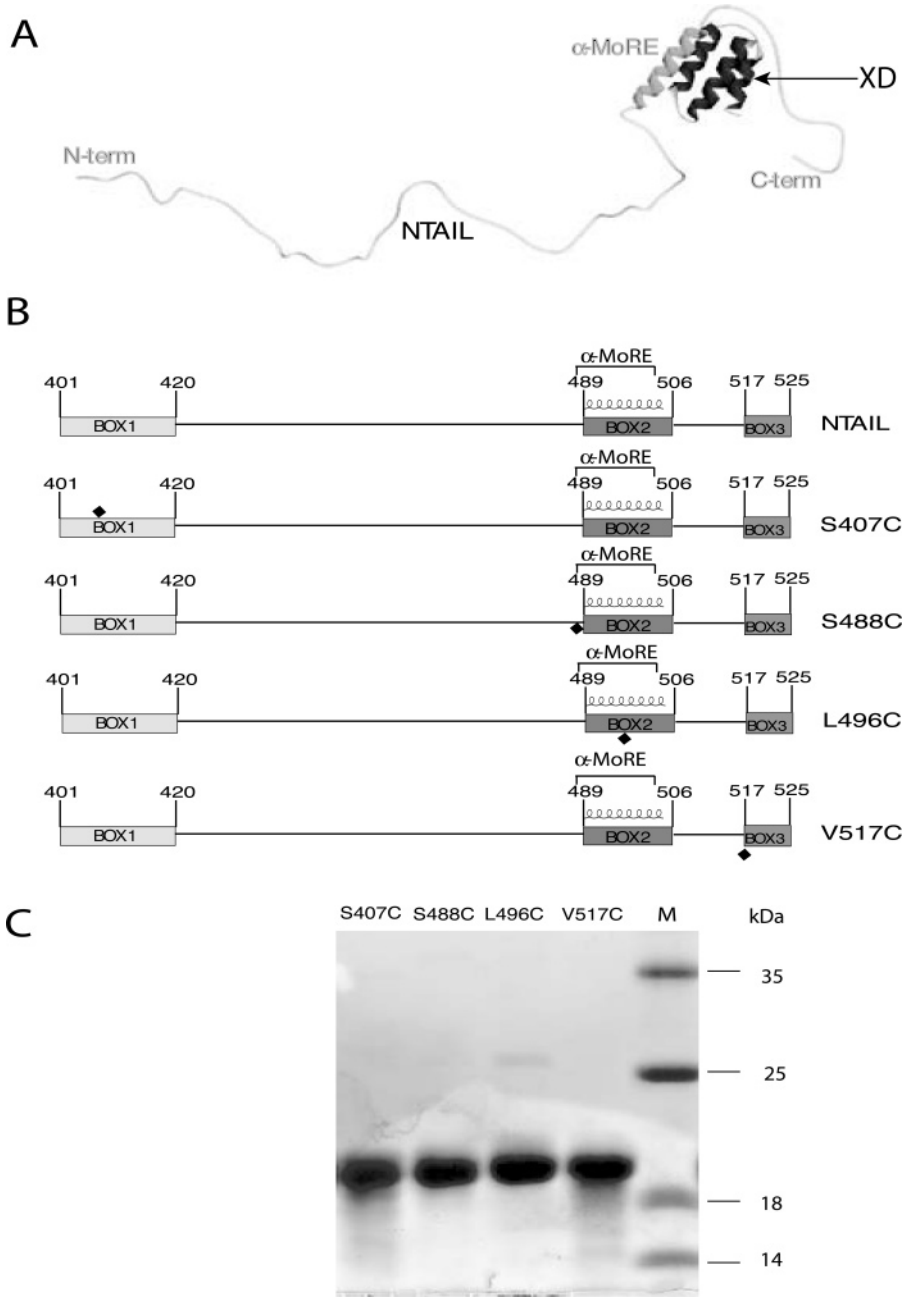

Figure 1. (A) Model of the N_{TAIL}−XD complex as derived by small-angle X-ray scattering studies, highlighting the involvement of the α-MoRE (Box2) and of the C-terminus of N_{TAIL} (Box3) in the interaction with XD.[31] **(B)** Schematic representation of N_{TAIL} mutated proteins. The positions targeted for the cysteine substitutions and spin-labeling are highlighted by black diamonds. **(C)** Purification of N_{TAIL} mutated proteins from *E. coli*. Coomassie blue staining of a 12% SDS−PAGE. M represents the molecular mass markers.

the crystal structure of a chimeric form of XD.[30] Using small-angle X-ray scattering, we have derived a low-resolution structural model of the complex between XD and N_{TAIL}. This model shows that most of N_{TAIL} (residues 401−488) remains disordered in the complex and does not establish contacts with XD, contrary to the 489−525 region of N_{TAIL}[31] (Figure 1A). Using surface plasmon resonance and various spectroscopic approaches, we have shown that, beyond the α-MoRE, N_{TAIL} has an additional site (Box3, aa 517−525) involved in binding to XD (Figure 1A); however, contrary to Box2 that undergoes α-helical folding upon binding to XD, the C-terminus of N_{TAIL} does not gain any regular secondary structure[31] (for reviews, see refs 32 and 33).

Electron paramagnetic resonance (EPR) spectroscopy is a technique that specifically detects unpaired electrons. EPR-sensitive reporter groups (spin labels or spin probes) can be introduced into biological systems via site-directed spin-labeling (SDSL). The basic strategy of SDSL involves the introduction of a paramagnetic nitroxide side chain at a selected protein site. This is usually accomplished by cysteine-substitution mutagenesis, followed by covalent modification of the unique sulfhydryl group with a selective nitroxide reagent, such as the methanethiosulfonate (MTSL) derivative (for reviews, see refs 34−36). SDSL EPR spectroscopy is a technique used to study conformational changes within structured proteins.[37] Although relatively high protein concentrations (usually $>10\ \mu$M) are required for acceptable signal-to-noise ratios of the resulting EPR spectra, this method is highly sensitive to conformational transitions within the vicinity of the spin labels and therefore allows the monitoring of conformational processes during substrate binding

and often during enzymatic turnover. Furthermore, the relatively small size of the spin label (~7 Å) was shown not to perturb the biological activity of the enzyme or protein in several studies (for examples see, refs 34, 38, and 39).

SDSL followed by EPR spectroscopy has been extensively used to study folding and unfolding processes of structured proteins in the presence of denaturing agents, such as urea and guanidium chloride.[40,41] Accordingly, we reasoned that this technique could also be well-suited to assess induced folding events, i.e., disorder-to-order transitions experienced by IDPs upon binding to their physiological partners.[9,42−46] These disorder-to-order transitions can be accompanied by the gain of regular secondary structure elements.[6,31,44,45,47] Therefore, the term induced folding is herein used to designate all disorder-to-order transitions that IDPs undergo upon binding to their partner/ligand, regardless of whether they imply α- or β-transitions.

We evaluated the ability of SDSL EPR spectroscopy to monitor the induced folding of the intrinsically unstructured C-terminal domain of the MV nucleoprotein, N_{TAIL}, in the presence of the C-terminal X domain of the phosphoprotein. To this endeavor, we targeted for spin-labeling four different sites within N_{TAIL}, one falling in the N-terminal region (Box1, position 407), one located immediately upstream of the α-MoRE (position 488), one within the α-MoRE (position 496), and the fourth in the C-terminus (Box3, position 517) (Figure 1). We then monitored the variations in the mobility of the spin label upon addition of either the secondary structure stabilizer 2,2,2-trifluoroethanol (TFE) or the physiological partner, XD.

We show that SDSL EPR spectroscopy is a well-suited method to monitor the induced folding events that N_{TAIL} undergoes in the presence of TFE or XD, while providing information at the residue level. Therefore, it can be added to the panel of widely used experimental approaches to study induced folding events (reviewed in ref 48).

Materials and Methods

Bacterial Strains and Media. The *Escherichia coli* strain DH5α (Stratagene) was used for selection and amplification of DNA constructs. The *E. coli* strain Rosetta [DE3] pLysS (Novagen) was used for expression of recombinant proteins. *E. coli* were grown in Luria-Bertani (LB) medium.

Construction of Protein Expression Plasmids. The XD gene construct, encoding residues 459−507 of the measles virus P protein (strain Edmonston B) with an hexahistidine tag fused to its C-terminus, has already been described.[27]

All N_{TAIL} constructs were obtained by polymerase chain reaction (PCR) using the plasmid pDest14/N_{TAILHN},[31] which encodes residues 401−525 of the MV N protein (strain Edmonston B) with a hexahistidine tag fused to its N-terminus, as a template. Each mutant construct was obtained using Turbo-Pfu polymerase (Stratagene) and a pair of complementary mutagenic primers (Invitrogen). PCR cycles were carried out according to the supplier's instructions. After digestion with *Dpn*I to remove the methylated DNA template, transformation of *E. coli* with the amplified PCR product was carried out. The N_{TAIL} S407C gene construct, encoding residues 401−525 of the MV N protein with a Ser → Cys substitution at position 407 of N and with a N-terminal hexahistidine tag, was obtained using forward (5′-actactgaggacaagatc***TgC***agagcggttggacccaga) and reverse (5′- tctgggtccaaccgct***ctGcA***gatcttgtcctcagtagt) primers. The N_{TAIL} S488C gene construct, encoding residues 401−525 of the MV N protein with a Ser → Cys substitution at position 488 of N and with a N-terminal hexahistidine tag, was obtained using forward (5′-agccaagatccgcaggac***Tgc***AgAaggtcagctgacgcc) and reverse (5′-ggcgtcagctgacctTc***Tgc***Agtcctgcggatcttggct) primers. The N_{TAIL} L496C gene construct, encoding residues 401−525 of the MV N protein with a Leu → Cys substitution at position 496 of N and with a N-terminal hexahistidine tag, was obtained using forward (5′-aggtcagctgacgccct***CTGCag***gctgcaagccatggca) and reverse (5′-tgccatggctgcagc***ctGCA***Gagggcgtcagctgacct) primers. The N_{TAIL} V517C gene construct, encoding residues 401−525 of the MV N protein with a Val → Cys substitution at position 517 of N and with a N-terminal hexahistidine tag, was obtained using forward (5′-gacacggacaccccc***CataTGT***tacaatgacagaaatctt) and reverse (5′-aagatttctgtcattgta***ACA***tat***G***ggggtgtccgtgtc) primers. Upper-case nucleotides correspond to mismatches. All couples of primers were designed to introduce a Cys codon (bold), as well as either a *Pst*I (N_{TAIL} S407C, N_{TAIL} S488C, and N_{TAIL} L496C gene constructs) or a *Nde*I (N_{TAIL} V517C gene construct) restriction site (italic) for discrimination of candidate clones from parental (*Dpn*I-undigested) clones after transformation. The sequence of the coding region of all expression plasmids was verified by sequencing (MilleGen).

Expression of N_{TAIL} Constructs. *E. coli* strain Rosetta [DE3] (Novagen) was used for the expression of N_{TAIL} mutants. Since the MV N gene contains several rare codons that are used with a very low frequency in *E. coli*, coexpression of N_{TAIL} constructs with the plasmid pLysS (Novagen) was carried out. This plasmid, which supplies six rare tRNAs, also carries the lysozyme gene, thus allowing a tight regulation of the expression of the recombinant gene as well as a facilitated lysis. Cultures were grown overnight to saturation in LB medium containing 100 μg/mL ampicilin and 17 μg/mL chloramphenicol. An aliquot of the overnight culture was diluted 1:25 in LB medium and grown at 37 °C. At an OD_{600} of 0.7, isopropyl-β-D-thiogalactopyranoside (IPTG) was added to a final concentration of 0.2 mM, and the cells were grown at 37 °C for 3 h. The induced cells were harvested, washed, and collected by centrifugation. The resulting pellets were frozen at −20 °C.

Expression of tagged XD was carried out as described in ref 27. Expression of hexahistidine-tagged wild-type (wt) N_{TAIL} (N_{TAILHN}) was carried out as described in ref 31.

Purification of N_{TAIL} Protein Variants. Cellular pellets from bacteria transformed with the different N_{TAIL} expression plasmids were resuspended in 5 volumes (v/w) of buffer A (50 mM sodium phosphate at pH 8, 300 mM NaCl, 10 mM imidazole, 1 mM phenyl-methyl-sulfonyl-fluoride (PMSF)) supplemented with lysozyme 0.1 mg/mL, DNAse I 10 μg/mL, and a protease inhibitor cocktail (Sigma) (50 μL/g cells). After a 20 min incubation with gentle agitation, the cells were disrupted by sonication (using a 750 W sonicator and 4 cycles of 30 s each at 60% power output). The lysate was clarified by centrifugation at 30 000 g for 30 min. Starting from a 1 L culture, the clarified supernatant was incubated for 1 h with gentle shaking with 4 mL of Chelating Sepharose Fast Flow Resin preloaded with Ni^{2+} ions (Amersham Pharmacia Biotech), previously equilibrated in buffer A. The resin was washed with buffer A containing 20 mM imidazole, and the N_{TAIL} proteins were eluted in buffer A containing 250 mM imidazole. Eluates were analyzed by sodium dodecyl sulfate polyacrylamide gel electrophoresis (SDS-PAGE) for the presence of the desired product. The fractions containing the recombinant product were combined and concentrated using Centricon Plus-20 (molecular cutoff 5000 Da) (Millipore). The proteins were then loaded onto a Superdex 75 HR 10/30 column (Amersham Pharmacia Biotech) and eluted in 10 mM sodium phosphate pH 7. The

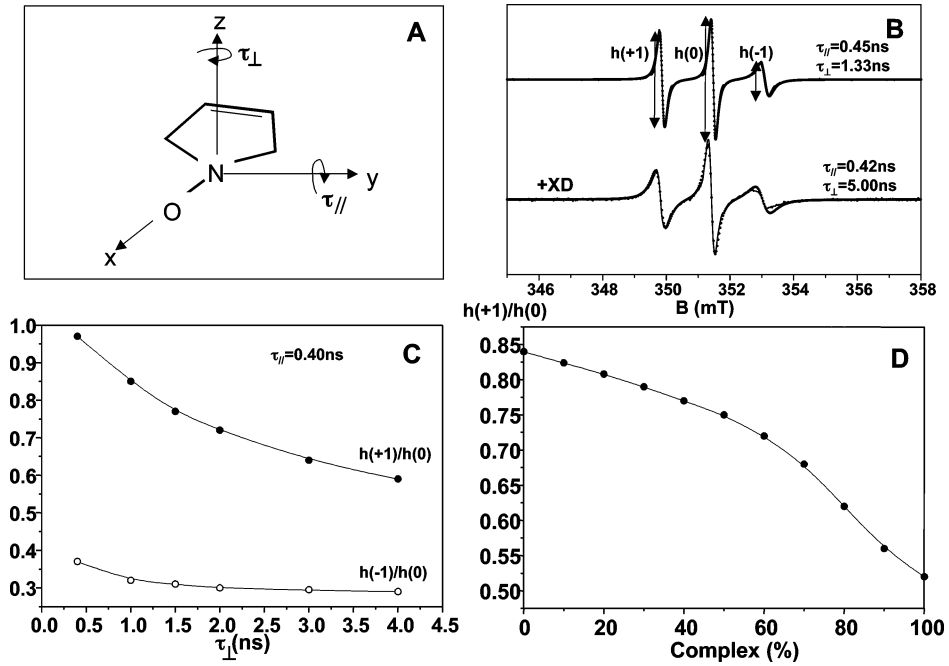

Figure 2. (A) Magnetic axes of MTSL. The *x*-axis is directed along the N−O bond, and the *z*-axis is perpendicular to the C−NO−C plane. (B) Simulated (dotted line) and experimental (solid line) spectra of labeled S488C free and in interaction with XD (molar excess of 2:1). The rapid movement of the spin label is taken around the *y*-axis. $h(+1)$, $h(0)$, and $h(-1)$ are the peak-to-peak amplitudes of the low-field, central-field, and high-field lines of the spectrum, respectively. **(**C**)** Variation of the $h(+1)/h(0)$ ratio (●) and $h(-1)/h(0)$ ratio (○) vs $\tau_\perp$ as deduced from simulated spectra. $\tau_{||}$ has a constant value of 0.4 ns. **(**D**)** Variation of $h(+1)/h(0)$ vs the percentage of spin-labeled S488C bound to XD.

proteins were stored at −20 °C. The purified N_{TAIL} proteins with a hexahistidine tag fused at the N-terminus bearing either the S407C, S488C, L496C, or V517C substitutions are referred to as S407C, S488C, L496C and V517C, respectively.

Purification of histidine-tagged XD and wt N_{TAIL} was carried out as described in refs 27 and 31.

All purification steps, except for gel filtrations, were carried out at 4 °C. The apparent molecular mass of proteins eluted from gel filtration columns was deduced from a calibration carried out with low molecular weight (LMW) and high molecular weight (HMW) calibration kits (Amersham Pharmacia Biotech). The theoretical Stokes radii (R_S) of a native (R_SN) and fully unfolded (R_SU) protein were calculated according to:[49] $\log(R_S\text{N}) = 0.369 \log(\text{MM}) - 0.254$ and $\log(R_S\text{U}) = 0.533 \log(\text{MM}) - 0.682$, with (MM) being the molecular mass (in daltons) and R_S being expressed in angstroms.

Determination of Protein Concentration. Protein concentrations were either calculated using OD_{280} measurements and the theoretical absorption coefficients ϵ (mL mg^{-1} cm^{-1}) at 280 nm as obtained using the program ProtParam at the EXPASY server (http://www.expasy.ch/tools) or measured using the Biorad protein assay (Bio-Rad).

Spin-Labeling. Before spin-labeling, dithiothreitol (DTT) was added to each purified N_{TAIL} mutated protein (approximately 5 mg) in a molar excess of 1:1000. The mixture was incubated for 30 min in an ice bath to reduce the unique free cysteine residue. DTT was removed by gel filtration onto a Superdex 75 HR 10/30 column (Amersham Pharmacia Biotech) with 10 mM MES, 150 mM NaCl at pH 6.5 as elution buffer. The fractions containing the protein were pooled and then concentrated by ultrafiltration using a 5 kDa cutoff polyethersulfone membrane (Vivaspin, Sartorius). The spin label 1-oxyl-2,2,5,5-tetramethyl-δ3-pyrroline-3-methyl (MTSL) (Toronto Research Chemicals, Inc., Toronto, Canada) was immediately added to the concentrated sample at a molar excess of 10:1 using a spin label stock solution at 10 mg/mL in acetonitrile. The reaction was carried out during 1 h in the dark in an ice bath, under gentle stirring and a continuous flow of nitrogen to avoid oxidation. The excess of unbound spin label was removed by gel filtration as described above, except that 10 mM sodium phosphate at pH 7 was used as the elution buffer. The fractions giving an EPR signal of labeled proteins were pooled and concentrated as described above.

EPR Spectroscopy. EPR spectra were recorded at room temperature on an ESP 300E Bruker spectrometer equipped with an ELEXSYS super high sensitivity resonator operating at 9.9 GHz. Samples were injected in a quartz capillary, whose sensible volume was about 20 μL. The microwave power was 10 mW, and the magnetic field modulation frequency and amplitude were 100 kHz and 0.1 mT, respectively.

The concentration of labeled proteins was evaluated by double integration of the EPR signal recorded under nonsaturating conditions and comparison with that given by a $CuSO_4$ standard sample. The labeling yields were estimated by calculating the ratio between the concentration of labeled proteins and the total protein concentration estimated as described above. Labeling yields were estimated to be 80% in the case of S488C, L496C, and V517C and to be 46% in the case of S407C.

Protein concentrations of either 20 or 40 μM were used to record individual EPR spectra in the presence of 8 M urea or of TFE (Fluka) concentrations ranging from 0% to 40% or of a 2-fold molar excess of XD. Experiments in the presence of 30% (w/v) sucrose were carried out using protein concentrations of 20 μM.

Equilibrium displacement experiments were carried out with 20 μM of spin-labeled protein sample, 40 μM of XD, and 20 μM of either unlabeled S407C or wt N_{TAIL} to yield 1:2:1 protein mixtures. We have checked that the proportion of unlabeled S488C and L496C (20%) has no impact on the observed equilibrium shift.

Simulation of EPR Spectra. The spin Hamiltonian of a frozen solution of nitroxide radical is $H = \beta\vec{B}\tilde{g}\vec{S} + \vec{S}\tilde{A}\vec{I}$. The

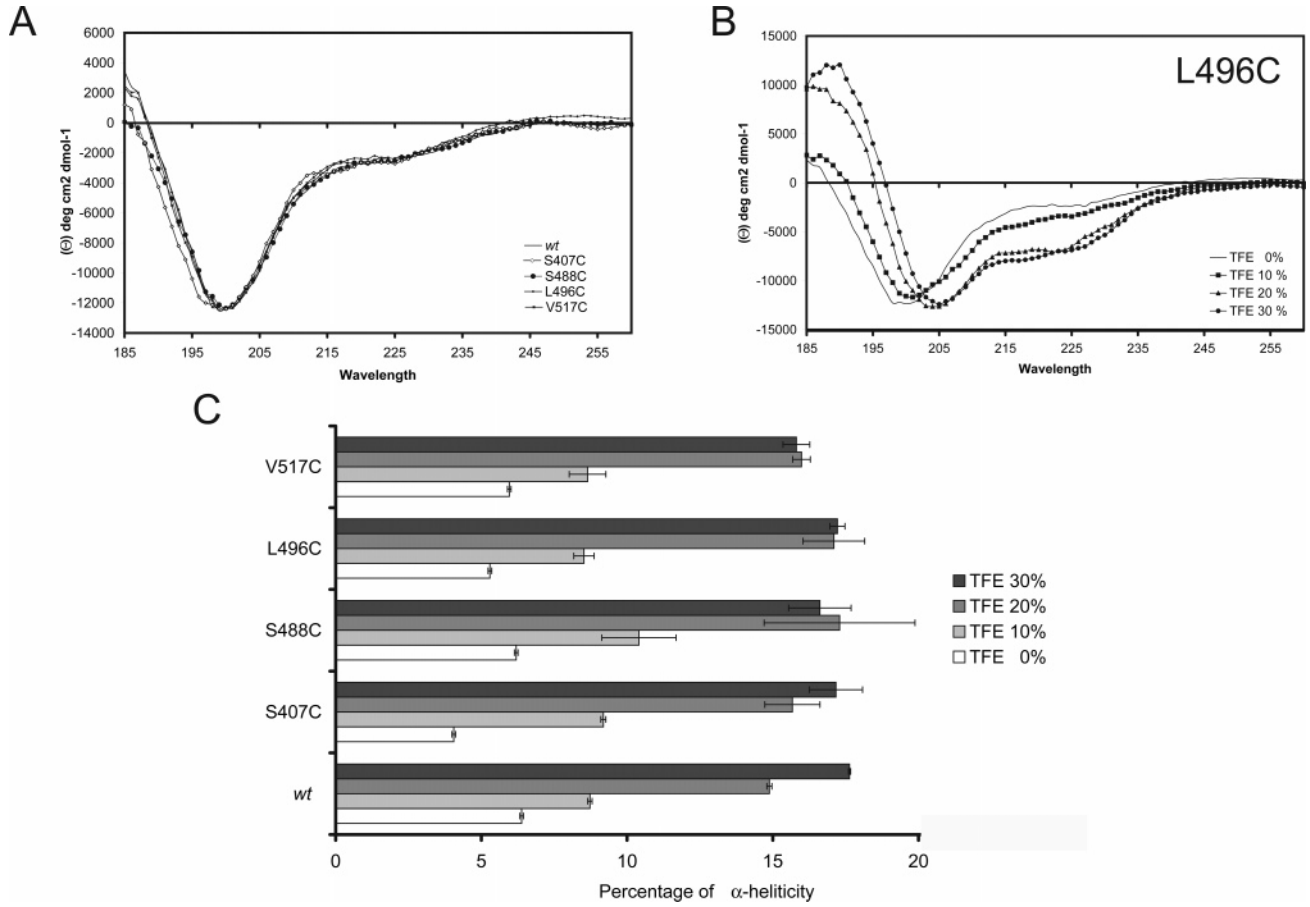

Figure 3. (A) Far-UV CD spectra of spin-labeled and wt N_{TAIL} proteins at 0.1 mg/mL in 10 mM sodium phosphate at pH 7 recorded at 20 °C. Each spectrum is the mean of three independent acquisitions. **(**B**)** Far-UV CD spectra of spin-labeled L496C N_{TAIL} at 0.1 mg/mL in the presence of increasing TFE concentrations. **(**C**)** α-Helical content of the spin-labeled and wt N_{TAIL} proteins at different TFE concentrations.

first term represents the interaction of the impaired electron with the static field (Zeeman interaction), and the second term describes the hyperfine interaction between this impaired electron and the ^{14}N nuclear spin. The simulation of the frozen samples is required to determine the three components of the $\tilde{g}$ and $\tilde{A}$ tensors. It was achieved by first obtaining the exact energies given by the above Hamiltonian and then by calculating the resonant fields and the corresponding probabilities of transition for all the orientations of the static field $\vec{B}$ with respect to the $\tilde{g}$ and $\tilde{A}$ principal axes. (The $\tilde{g}$ and $\tilde{A}$ axes were taken to be parallel.) The Lorentzian line width of a transition results from the convolution of a residual broadening (due to unresolved hyperfine coupling and finite lifetime of energy states) and a *g*-strain broadening.[50]

At room temperature, the experimental EPR spectra of the spin-labeled N_{TAIL} proteins are composed of three lines, with the width of them indicating that the spin label has a rapid and anisotropic rotational movement. The description of this fast anisotropic rotation can be done by considering a rapid movement of the spin label around an axis characterized by the rotational correlation time $\tau_{||}$ and a slower movement around an axis normal to the previous one, characterized by the rotational correlation time $\tau_{\perp}$ (Figure 2A).[51,52]

The simulation of the room-temperature EPR spectra of spin-labeled N_{TAIL} was obtained via the same procedure used for the simulation of its frozen solution (diagonalization of a Hamiltonian, determination of the resonant magnetic field and of the transition probabilities, and evaluation of the line width of each transition line). In this case, the spin Hamiltonian used is $H = g\beta\vec{B}\vec{S} + A\vec{S}\vec{I}$, where

$$g = \frac{1}{3}(g_x + g_y + g_z) \quad \text{and} \quad A = \frac{1}{3}(A_x + A_y + A_z)$$

The Lorentzian line width of the three motional averaged ^{14}N hyperfine lines is given by $\Delta B = A' + A + Bm_I + Cm_I^2$ where m_I is the nuclear quantum magnetic number of ^{14}N. The line width coefficients *A*, *B*, and *C* are related to the rotational correlation times $\tau_{||}$ and $\tau_{\perp}$ and the $\tilde{g}$ and $\tilde{A}$ anisotropies.[52] A' is the residual width obtained for a very high mobility of the spin label. Its value is due to all the isotropic contributions to the line width of the spin label that may occur.

Circular Dichroism. Circular dichroism (CD) spectra were recorded on a Jasco 810 dichrograph using 1-mm-thick quartz cells in 10 mM sodium phosphate at pH 7 at 20 °C.

Structural variations of N_{TAIL} proteins were measured as a function of changes in the initial CD spectrum upon addition of increasing concentrations of TFE. CD spectra were measured between 185 and 260 nm at 0.2 nm/min and were averaged from three independent acquisitions. The spectra were corrected for buffer signal and smoothed by using a third-order least-squares polynomial fit. Finally, mean ellipticity values per residue ($[\Theta]$) were calculated as $[\Theta] = 3300m\Delta A/(lcn)$, where *l* (path length) = 0.1 cm, *n* = number of residues, *m* = molecular mass in daltons, and *c* = protein concentration expressed in mg/mL. The number of residues (*n*) is 132 for all N_{TAIL} proteins, while *m* values are 15 627 Da for wt N_{TAIL}, 14 648 Da for S407C and S488C, 14 622 Da for L496C, and 14 632 Da for V517C. Protein concentrations of 0.1 mg/mL were used. The α-helical content was derived from the ellipticity at 220 nm as described in ref 53.

Results

Cloning, Expression, and Purification of N_{TAIL} Mutants. N_{TAIL} contains three regions of homology conserved among members of the *Morbillivirus* genus.[54] These regions are referred to as Box1, Box2, and Box3 and span residues 401−420, 489−506, and 517−525 of N, respectively (Figure 1B), with the α-MoRE being located within Box2. We have previously shown that Box2 and Box3 are both involved in the interaction with XD, while Box1 is not[31] (Figure 1A).

We have designed four individual cysteine mutants, thus allowing introduction of the spin label at four different locations within N_{TAIL} (Figure 1B). Specifically, we targeted Box1 (position 407), two positions either close to or within Box2 (positions 488 and 496, respectively), and Box3 (position 517). Whenever possible, serine to cysteine substitutions were done. In the case of Box1, Ser407 was targeted for site-directed mutagenesis, as this residue is not conserved within *Morbillivirus* members, contrary to Ser418.[54] We also targeted Ser488, which is located at the beginning of the α-MoRE, rather than Ser491. The rationale for this choice comes from the visual inspection of the crystal structure of the complex between XD and the α-MoRE of N_{TAIL} (PDB code 1T6O),[30] which shows that the side chain of Ser488 points toward the solvent, whereas that of Ser491 is buried at the interface of interaction. As the introduction of the nitroxide radical at position 491 might hinder the interaction with XD, we targeted position 488 for cysteine substitution. To target a position occurring in the middle of the α-MoRE, we selected Leu496 for isosteric cysteine substitution because the side chain of Leu 496, like that of Ser488, points toward the solvent in the complex between XD and the α-MoRE. Finally, as no serine residue occurs within Box3, Val517 was chosen for isosteric cysteine substitution (Figure 1B).

All recombinant N_{TAIL} proteins were expressed in *E. coli* and were recovered from the soluble fractions of the bacterial lysates (data not shown). The N_{TAIL} mutated proteins were purified to homogeneity (>95%) in two steps: immobilized metal affinity chromatography and gel filtration. As shown in Figure 1C, the four N_{TAIL} mutated proteins migrate in SDS-PAGE with an apparent MM of 20 kDa. (The expected MM is approximately 14.6 kDa.) This abnormal migratory behavior has already been documented for N_{TAIL}, where mass spectrometry analysis and N-terminal sequencing gave the expected results.[15] The anomalous electrophoretic mobility is therefore due to a rather high content of acidic residues, as frequently observed in other IDPs,[2] such as, for instance, in the DNA repair protein XPA.[55] Likewise, the behavior of the mutated N_{TAIL} proteins can be accounted for by this sequence bias.

The number of different conformations of the N_{TAIL} mutated proteins is limited, as indicated by the sharpness of the peaks observed in gel filtration (data not shown). The Stokes radius (R_S) value of the N_{TAIL} mutated proteins, as inferred by gel filtration (27 ± 3 Å), is not consistent with the theoretical values (19 ± 3 Å) expected for globular conformations (see Materials and Methods). Rather, the corresponding hydrodynamic volume value (comprised between 85 000 and 97 000 Å^3, as inferred from the R_S) is consistent with the theoretical value (about 94 000 Å^3) expected for a premolten globule state,[3] as already observed in the case of wt N_{TAIL}.[15] Thus, these mutated proteins share similar hydrodynamic properties with wt N_{TAIL}, being nonglobular while possessing a certain residual compactness typical of the premolten globule state.[49]

Circular Dichroism Analysis of N_{TAIL} Variant Proteins. To assess whether the cysteine substitutions and/or the introduction of the covalently bound nitroxide radical affect the overall secondary structure of N_{TAIL}, we recorded far-UV CD spectra of either spin-labeled or unlabeled mutated N_{TAIL} proteins at neutral pH. Figure 3A shows the CD spectra of spin-labeled and wt N_{TAIL} proteins, which are all typical of unstructured proteins, as seen by their large negative ellipticity at 198 nm and very low ellipticity at 185 nm. The CD spectra of unlabeled mutated proteins superimpose quite well onto those of spin-labeled proteins (data not shown). As already observed in the case of wt N_{TAIL},[15] the ellipticity values at 200 and 222 nm are consistent with the existence of some residual, transient secondary structure typical of the premolten globule state.[3] Notably, all the obtained CD spectra superimpose well onto the CD spectrum of wt N_{TAIL}, thus indicating that the mutations and the presence of the spin label do not affect the overall secondary structure content of the variant N_{TAIL} proteins (Figure 3A and data not shown).

The solvent TFE mimics the hydrophobic environment experienced by proteins in protein−protein interactions and is therefore widely used as a probe to unveil disordered regions having a propensity to undergo an induced folding.[56] We have previously reported that the addition of increasing amounts of TFE to N_{TAIL} triggers an increase in the α-helicity of this protein and that Box2/α-MoRE plays a major role in this random coil to α-helix transition.[15,29,31] To ascertain that the introduction of the mutation and of the nitroxide radical does not affect the folding propensities of N_{TAIL}, we have recorded CD spectra of spin-labeled N_{TAIL} proteins in the presence of increasing concentrations of TFE (Figure 3B and data not shown). All proteins show a similar increasing gain of α-helicity upon addition of TFE, as indicated by the characteristic maximum at 190 nm and minima at 208 and 222 nm (Figure 3B and data not shown). From the ellipticity value at 222 nm, we calculated the α-helical content of each protein at the various TFE concentrations (Figure 3C). The four spin-labeled proteins share similar α-helical propensities and have α-helical contents consistent with those already reported for wt N_{TAIL}.[15,29,31]

These results indicate that the mutation and the presence of the spin label at four distinct positions do not affect the structural propensities of N_{TAIL}.

EPR Data Analysis of Spin-Labeled N_{TAIL} Proteins. The shapes of all the free spin-labeled N_{TAIL} spectra obtained in this study are characteristic of a fast anisotropic movement of the nitroxide group. $\tau_{||}$ and $\tau_{\perp}$ correlation times were determined from the simulation of the EPR spectra (see Materials and Methods). First, the g and hyperfine tensors elements g_{ii} and A_{ii} ($i = x,y,z$) were obtained by simulating the spectrum of a frozen solution (150 K) of the spin-labeled protein. Second, the $\tau_{||}$ and $\tau_{\perp}$ rough values were estimated from the broadening of the room-temperature spectrum lines as compared to those of the free label in solution. Then, the room-temperature spectrum was simulated by refining the $\tau_{||}$ and $\tau_{\perp}$ values. An example of simulated spectra of spin-labeled S488C N_{TAIL} free and in interaction with XD, which affects the mobility of the radical and thus the values of $\tau_{||}$ and $\tau_{\perp}$, is shown in Figure 2B. The good agreement between simulated and experimental spectra allowed the determination of the magnetic parameters and correlation times with confidence (Table 1). As it is seen, the spectral changes are essentially due to the increase of $\tau_{\perp}$. Interestingly, the analysis of these spectral changes (Figure 2B) shows that the ratio of the peak-to-peak amplitudes of the low field and central field lines (named $h(+1)/h(0)$ herein after) varies from 0.83 to 0.50 when N_{TAIL} is in interaction with its partner (see Table 1 and below).

TABLE 1: Magnetic Parameters and Correlation Times Obtained from Simulation of EPR Spectra

protein sample	$\tau_{\|}$ (ns)	$\tau_{\perp}$ (ns)	$h(+1)/h(0)$
S488C	0.45	1.33	0.83
S488C−XD	0.42	5.00	0.50
g-tensor	$g_x = 2.0086$	$g_y = 2.0060$	$g_z = 2.0024$
A-tensor (Gs)	$A_x = 5.6$	$A_y = 5.6$	$A_z = 36.7$

To show that the $h(+1)/h(0)$ ratio can be used as a direct indicator of the spin label mobility, its variation as a function of typical rotational correlation times encountered in our experiments was deduced from simulated spectra (Figure 2C). As shown in Figure 2C, the $h(+1)/h(0)$ ratio significantly varies as a function of correlation time. This approach has the advantage of being much more direct as compared to the simulation procedure. Moreover, the $h(+1)/h(0)$ ratio is a better suited and more sensitive parameter than the $h(-1)/h(0)$ ratio (Figure 2B) to infer information about the radical mobility, as illustrated in Figure 2C, where variations in the $h(-1)/h(0)$ ratios are approximately 4 times smaller than variations in the $h(+1)/h(0)$ ratios for a given variation of $\tau_{\perp}$. Note that for isotropic movements of the label the behavior of both ratios is reversed: $h(-1)/h(0)$ varies significantly whereas $h(-1)/h(0)$ is almost stable.[41,57]

The measurement of the $h(+1)/h(0)$ ratio also allowed us to infer the percentage of spin-labeled N_{TAIL} protein bound to XD in unsaturated complexes, i.e., where only a fraction of spin-labeled N_{TAIL} is bound to XD (Figure 2D, and the subsection "Equilibrium Displacement Experiments"). This percentage is deduced from the $h(+1)/h(0)$ ratio variation versus the percentage of the spin-labeled N_{TAIL}−XD complex, which is obtained from the calculation of composite spectra corresponding to mixtures of simulated spectra of free and 100% XD-bound spin-labeled S488C (Figure 2D).

For all the spin-labeled N_{TAIL} proteins, the EPR spectra are indicative of a high radical mobility, as judged on the basis of the $h(+1)/h(0)$ ratio (ranging from 0.8 to 0.9) (Figure 4). Despite the overall high mobility, slight differences were observed in the different spin-labeled N_{TAIL} proteins. A fast and nearly isotropic movement is observed for the nitroxide radical covalently bound to positions 407 and 517 (i.e., the N- and C-terminal regions of N_{TAIL}), while an anisotropic and slower movement is observed for the nitroxide radicals covalently bound to positions 488 and 496 (Figure 4), as judged based on the $h(+1)/h(0)$ ratios. The mobility of the spin labels grafted at positions 407 and 517 in the presence of 8 M urea is not significantly different with respect to that obtained in native conditions. Conversely, the mobility of the spin labels bound at positions 488 and 496 is slightly higher under denaturing conditions as compared to native conditions (Figure 4).

Effect of TFE on Spin-Labeled N_{TAIL} Proteins. To evaluate the ability of SDSL EPR spectroscopy to monitor local folding events induced by TFE, we recorded EPR spectra of spin-labeled N_{TAIL} proteins in the presence of increasing concentrations of this secondary structure stabilizer (Figure 5).

In the case of the spin-labeled S407C protein, a TFE concentration as high as 20% is required to trigger a significant decrease of the mobility of the radical, with the $h(+1)/h(0)$ ratio shifting from 0.88 to 0.79 (±0.02). No further reduction in the mobility was observed upon addition of increasing TFE concentrations as high as 40%.

In the case of the spin-labeled S488C and L496C proteins, the addition of 10% TFE causes a significant reduction in the radical mobility, with the $h(+1)/h(0)$ shifting from 0.82 to 0.72 (±0.02) for S488C and from 0.83 to 0.74 (±0.02) for L496C. In both cases, further increasing the TFE concentration to 40% did not result in a further decrease in the mobility of the nitroxide radical.

In the case of the spin-labeled V517C protein, no significant reduction in the radical mobility was observed even at a TFE concentration of 40%.

The possibility that TFE might affect the mobility of the free radical in solution was checked and ruled out by comparing the EPR spectra obtained with a 40 μM MTSL nitroxide derivative solution in the presence or absence of 40% TFE (data not shown). The lack of intrinsic variations in the mobility of the free radical ensures that the observed variations in the radical mobility with the spin-labeled N_{TAIL} proteins reflect changes in the protein environment in the proximity of the spin label.

Altogether, these data indicate a different contribution of N_{TAIL} regions to the gain of rigidity induced by TFE, with effects ranging from null (Box3) to appreciable (Box2 and Box1).

Effect of XD on Spin-Labeled N_{TAIL} Proteins. To evaluate the ability of SDSL EPR spectroscopy to monitor folding events induced by the physiological partner XD, we recorded EPR spectra of spin-labeled N_{TAIL} proteins in the presence of a 2-fold molar excess of XD (80 μM) (Figure 6), a concentration well above the reported K_D (100 nM).[31]

In the case of the spin-labeled S407C protein, the addition of XD did not induce any modification in the radical mobility, even at XD molar excesses as high as 8:1 with respect to the concentration of the spin-labeled protein (Figure 6 and data not shown).

Conversely, in the case of the spin-labeled S488C and L496C proteins, the addition of a 2-fold molar excess of XD triggers a dramatic reduction in the radical mobility, with the $h(+1)/h(0)$ ratio shifting from 0.82 to 0.48 (±0.02) for S488C and from 0.83 to 0.47 (±0.02) for L496C.

Similarly, the addition of a 2-fold molar excess of XD to the spin-labeled V517C protein results in a significant reduction of the radical mobility, with the $h(+1)/h(0)$ ratio shifting from 0.89 to 0.79 (±0.02). However, this reduction (0.10 ± 0.02) is less pronounced as compared to that observed with the spin-labeled S488C and L496C proteins (0.34 and 0.36 (±0.02), respectively).

In all cases, a 2-fold molar excess of XD was required to achieve saturation of the complex, while the addition of stoichiometric amounts of XD led to only 80% complex (data not shown). In all cases, further increasing the XD concentration-to-molar ratios as high as 4:1 did not result in further reduction of the radical mobility (data not shown).

As a control, we recorded EPR spectra of a mixture containing spin-labeled S488C and a 2-fold molar excess of an irrelevant protein (lysozyme). No variation in the radical mobility was observed (data not shown), thus indicating that the reductions in the radical mobility observed with the S488C−XD, L496C−XD, and V517C−XD mixtures are specific of complex formation.

Altogether, these data indicate that the spin-labeled S488C, L496C, and V517C proteins interact with XD and that binding of XD affects the mobility of the nitroxide radicals bound at positions 488, 496, and 517.

Equilibrium Displacement Experiments. *Reversibility of Complex Formation.* To assess whether complex formation was a reversible process, we carried out equilibrium displacement experiments. We first recorded the EPR spectra of two mixtures containing either spin-labeled S488C or L496C and XD in a 1:2 molar ratio. Under these conditions, the percentage of the complex was estimated to be 100% (see Materials and Methods)

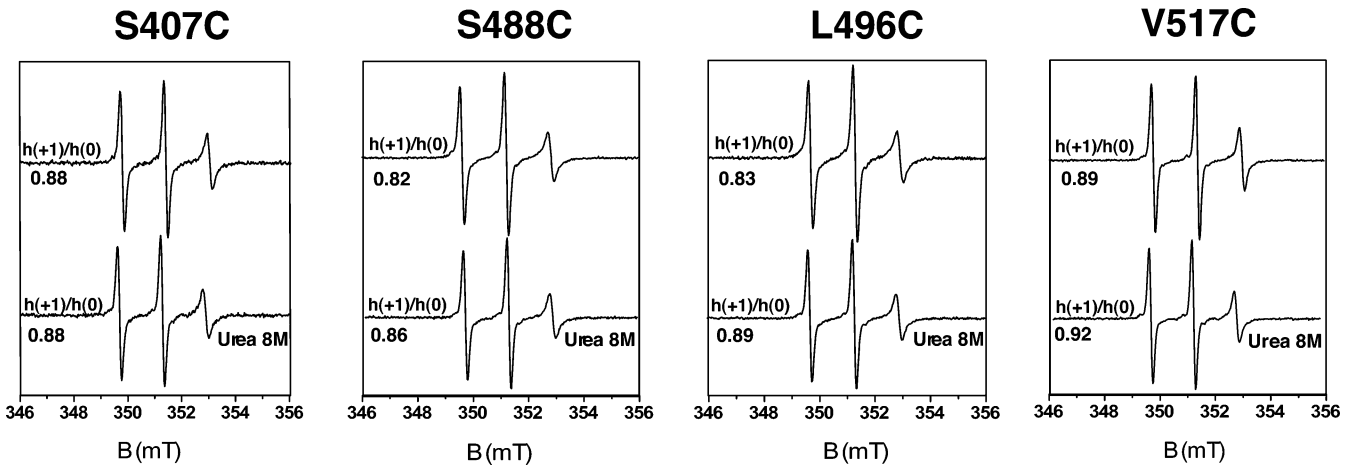

Figure 4. Normalized room-temperature EPR spectra of the four spin-labeled N_{TAIL} proteins in native conditions and in 8 M urea. The $h(+1)/h(0)$ ratios are shown.

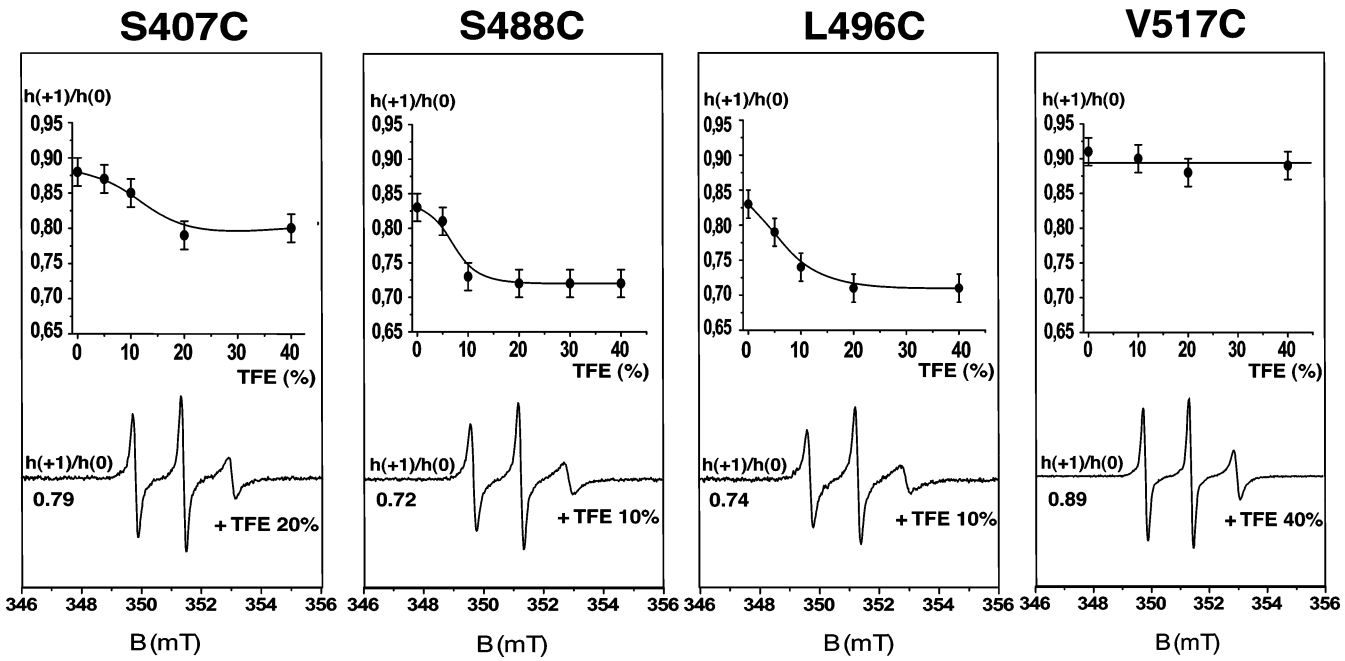

Figure 5. Normalized room-temperature EPR spectra of the four spin-labeled N_{TAIL} proteins at various TFE concentrations. The variations of the mobility of the nitroxide radical, expressed as variations of the $h(+1)/h(0)$ ratio, as a function of the TFE concentration are also shown.

(Figure 7). We then evaluated the ability of wt N_{TAIL} to displace the equilibrium toward the unbound forms of spin-labeled S488C and L496C. To this endeavor, we recorded the EPR spectra of two mixtures containing either spin-labeled S488C or L496C, XD, and wt N_{TAIL}, in a 1:2:1 ratio. The rationale for the choice of these molar ratios resides in the observation that the highest variations of the $h(+1)/h(0)$ occur in the range of percentages of $N_{TAIL}-$XD complex comprised between 60% and 100% (Figure 2D).

The spectra obtained in these experiments are composed of two signals: one arising from the free spin-labeled protein and one resulting from the spin-labeled protein bound to XD. The percentage of spin-labeled protein bound to XD was estimated as already described in the subsection "EPR Data Analysis of Spin-Labeled N_{TAIL} Proteins" (see also Figure 2D). The error in this determination was experimentally estimated to be 5%. With 1:2:1 ratios, the spectral changes show that the percentage of the spin-labeled S488C−XD and L496C−XD complexes decreases to 80% (±5%) (Figure 7). This decrease indicates that XD can dissociate from spin-labeled S488C and L496C and can associate with unlabeled wt N_{TAIL}, thus pointing out that complex formation is a reversible process. As a negative control, we recorded an EPR spectrum of a mixture containing spin-labeled S488C, XD, and lysozyme in a 1:2:1 ratio. No variation in the percentage of complex was observed (data not shown), reflecting lysozyme's inability to interact with XD and to displace the equilibrium.

Ability of S407C to Interact with XD. The lack of variations in the mobility of the spin label bound at position 407 upon addition of XD can be accounted for by assuming that either the mutated S407C protein has lost the ability to interact with XD or that the interaction does occur but does not affect the radical mobility because the label site is not located in the region of interaction. To discriminate between these two hypotheses, we checked whether the mutated S407C N_{TAIL} protein can displace the equilibrium of the $N_{TAIL}-$XD complex formation. We thus recorded the EPR spectrum of a mixture containing spin-labeled S488C, XD, and unlabeled S407C in a 1:2:1 ratio (data not shown). Under these conditions, the percentage of spin-labeled S488C−XD complex also decreased to 80% (±5%) (data not shown), thus confirming that the unlabeled S407C variant form is able to interact with XD and to shift the spin-

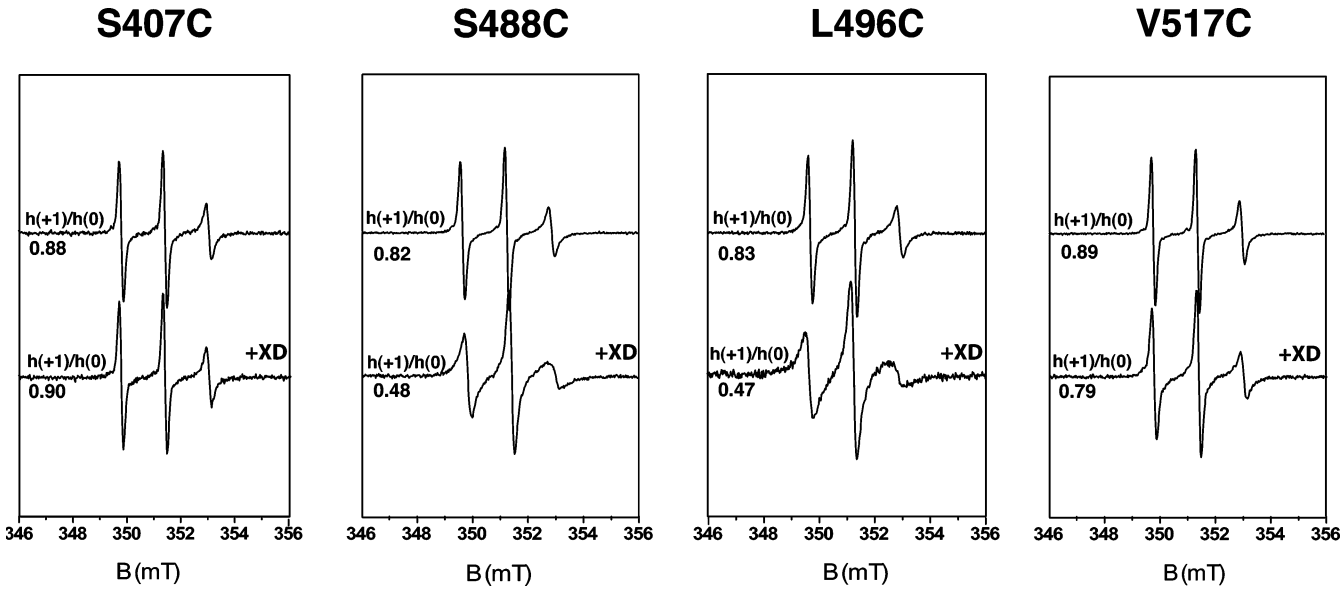

Figure 6. Normalized room-temperature EPR spectra of the four spin-labeled N_{TAIL} proteins in the absence or presence of a 2-fold molar excess of XD. The $h(+1)/h(0)$ ratios are indicated.

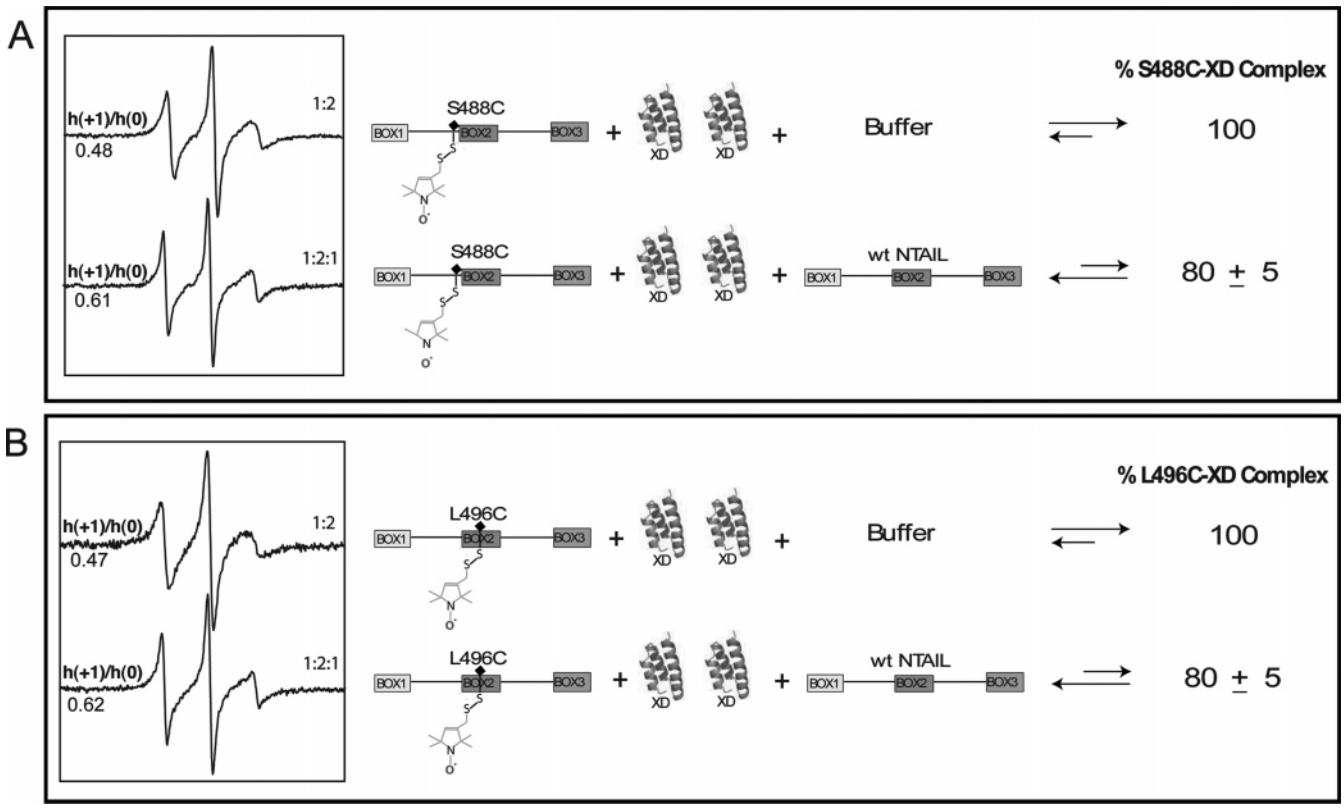

Figure 7. Dissociation of the spin-labeled S488C−XD and L496C−XD complexes by wt N_{TAIL}. Normalized room-temperature EPR spectra of the various mixtures are shown. Percentages of labeled S488C−XD and L496C−XD complexes in the different mixtures are given (see Materials and Methods), and the molar ratios are also indicated. Cysteine mutations have been represented by diamonds. The nitroxide radical is indicated. Note that the spacing between N_{TAIL} boxes does not reflect actual sizes.

labeled S488C−XD equilibrium toward the unbound form. Therefore the lack of reduction in the mobility of the radical bound at position 407 upon addition of a molar excess of XD points out the absence of the involvement of Box1 in the interaction with XD rather than the inability of the S407C N_{TAIL} protein to interact with its partner.

Mobility of the Spin Labels in the Presence of Sucrose. To further analyze the nature of the transition that the spin-labeled N_{TAIL} proteins undergo in the presence of XD, we recorded EPR spectra in the presence of 30% sucrose. Under these conditions, the contribution of protein rotation to the EPR spectral line shape is reduced due to an increase in the protein rotational correlation time by about a factor of 3. Moreover, it has been shown that the addition of 10−40% sucrose does not affect the rotational mobility of the side chain relative to the protein at room temperature.[38] The possibility that 30% sucrose might affect the overall secondary structure of the spin-labeled N_{TAIL} proteins was checked and ruled out by using CD (data not shown). As expected, the mobility of all spin labels was significantly reduced in the presence of sucrose (Figure 8)

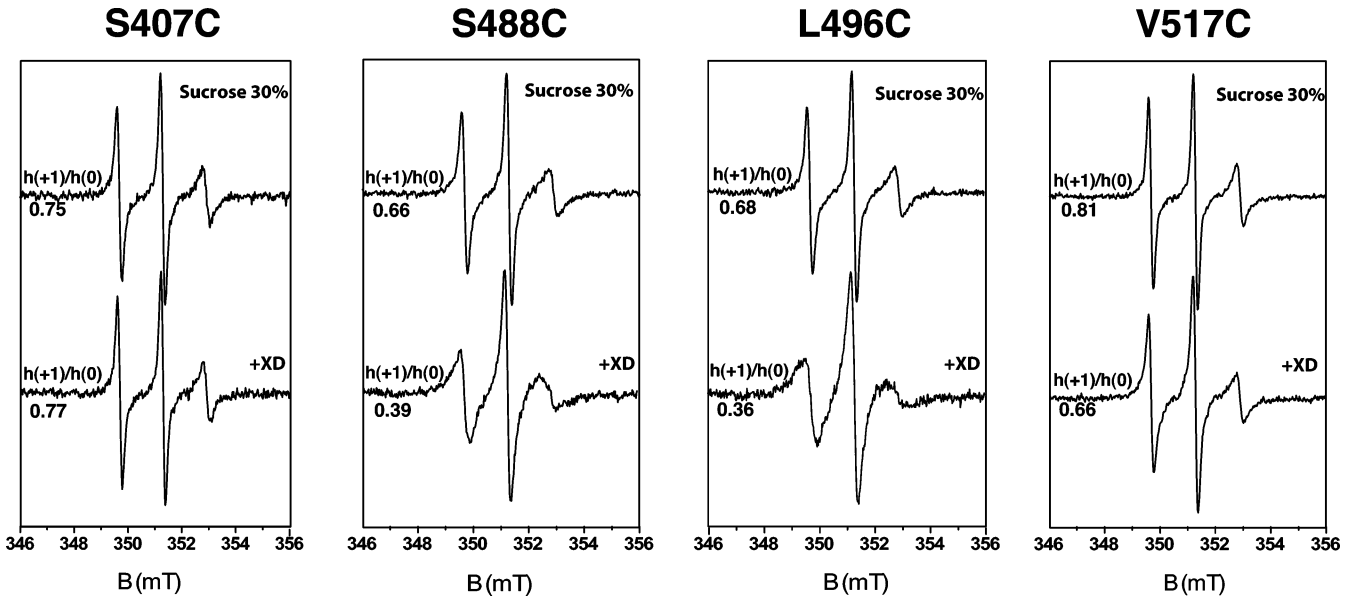

Figure 8. Normalized room-temperature EPR spectra of the four spin-labeled N_{TAIL} proteins in the presence of 30% sucrose and in the absence or presence of a 2-fold molar excess of XD. The $h(+1)/h(0)$ ratios are indicated.

regardless of the position of the spin label. The addition of a 2-fold molar excess of XD triggers a strong reduction in the radical mobility for the spin-labeled S488C, L496C, and V517C proteins, whereas it does not affect the mobility of the spin label grafted at position 407 (Figure 8). The most pronounced variation is observed for spin-labeled L496C (with a drop in the $h(+1)/h(0)$ ratio of 0.32), followed by S488C (with a drop of 0.27) and by V517C (with a drop of 0.15). The mobility of the nitroxide radicals of both spin-labeled S488C and L496C bound to XD is in the zone between the high and the intermediate regimes of mobility (with $\tau_{||} < 1$ ns).

Discussion

Residual Structure within N_{TAIL}. The $h(+1)/h(0)$ ratios observed for all spin-labeled N_{TAIL} proteins are indicative of a high mobility of the paramagnetic label. Nevertheless, slight mobility differences were observed in the different spin-labeled N_{TAIL} proteins (Figure 4). These minor differences could reflect either a higher inherent flexibility of the N- and C-terminal region of N_{TAIL} with respect to the central part of the protein or differences in the content of transient secondary structure elements in the local environment experienced by each label. This latter hypothesis is in agreement with previous observations pointing out that N_{TAIL}, while being an IDP, is not a (uniform) random coil but rather belongs to the premolten globule subfamily and thus possesses some residual and fluctuating secondary structure.[15,29] Accordingly, different regions within N_{TAIL} may display different extents of rigidity as a result of transient short-distance (secondary structure) or long-distance (tertiary structure) intramolecular interactions. The slightly higher mobility observed for spin-labeled S488C and L496C in denaturing conditions as compared to native conditions supports the existence of some residual secondary and/or tertiary structure in proximity to these positions. This may reflect the predominance of an α-helical conformation among the highly fluctuating conformations sampled by unbound N_{TAIL}, as shown by previous data that mapped the region involved in the α-helical induced folding to residues 489−506.[29] That the conformational space of MoREs [28] in the unbound state is restricted by their inherent conformational propensities, thereby reducing the entropic cost of binding, has already been proposed.[2,9−11,58]

TFE-Induced Folding of N_{TAIL}. In CD analyses, gradually increasing the TFE concentration from 10% to 30% triggers a progressive gain of α-helicity in all spin-labeled N_{TAIL} proteins (Figure 3C). Such experiments however only provide information about the overall α-helical content and do not provide indications about the location of the induced α-helices. Conversely, SDSL EPR spectroscopy allows a more precise mapping of TFE effects at different, targeted sites. Indeed, this method turned out to be sensitive only to structural changes occurring in close proximity to the spin label, with conformational changes taking place elsewhere in the protein not being detectable. This point is well illustrated by the observation that, although TFE induces an overall gain of α-helicity in spin-labeled V517C (Figure 3C), we cannot detect any variation of the mobility of the radical bound at position 517, even at high TFE concentrations (Figure 5). This indicates that TFE does not promote any structural transition in the environment close to residue 517 (i.e., Box3) and rather triggers gain of α-helicity in other N_{TAIL} regions. Indeed, the mobility of the radical at positions 488 and 496 is highly affected by TFE concentrations as low as 10% (Figure 5). This gain of rigidity can be accounted for by the α-helical transition of Box2 (aa 489−506), as already documented by previous spectroscopic studies.[29,31] It is noteworthy that the TFE-induced α-helical transition of Box2 does not affect the mobility of the radical bound at position 517, i.e., only 11 residues away from the C-terminus of this induced α-helix. This insensitiveness highlights the local nature of the information provided by this technique, which gives insights into the close neighborhood around the spin label.

The lack of a gain of α-helicity within Box3 upon addition of TFE is in agreement with previous spectroscopic studies, which showed that the C-terminus of N_{TAIL} does not affect the folding propensities of this protein and does not gain any regular secondary structure even upon binding to XD.[31] Notably, these data also point out the relevance of studies making use of TFE. Indeed, the reliability of structural information derived by CD studies in the presence of TFE is still a matter of debate, with artifactual (i.e., non-native) α-helical folding induced by this

solvent often being evoked.[59−61] However, the present results clearly indicate that even at a TFE concentration of 40% Box3 does not undergo α-helical folding, in agreement with conclusions derived from the study of the N_{TAIL}−XD complex.[31] Thus, in the case of N_{TAIL}, TFE does not seem to promote non-native folding, thus rendering biologically relevant structural information provided by studies making use of this secondary structure stabilizer.

In the case of Box1, a TFE concentration of 20% is required to trigger a reduction in the mobility of the radical at position 407 comparable to that observed in the case of the radical bound at positions 488 and 496 within Box2 (Figure 5). This indicates that TFE induces a gain of rigidity in the environment close to position 407 as well, thus suggesting that Box1 could be an additional N_{TAIL} region with a propensity to fold. Previous CD studies showed that TFE induces no structural transition within Box1.[31] The observed discrepancy between CD and EPR data obtained in the presence of TFE may be accounted for by assuming that TFE induces either an α-helical transition involving a limited number of residues, or a β-transition. These two types of structural transitions are both hardly detectable by CD,[62] thus explaining why the folding propensity of Box1 could have escaped detection so far. The biological relevance of the increased rigidity of Box1, as unveiled by SDSL EPR spectroscopy, may reside in a gain of structure possibly arising upon binding to a partner. Previous studies showed that Box1 is not involved in the interaction with XD.[31] However, we have previously shown that N_{TAIL} interacts with an extracellular receptor, the nucleoprotein receptor (NR), and that this interaction is mediated by Box1.[24] Therefore, we can speculate that Box1 could undergo induced folding upon binding to the NR. However, definitive answers on the gain of regular secondary structure elements by Box1 upon binding to NR await the isolation of this receptor and the molecular characterization of its interaction with N_{TAIL}.

XD-Induced Folding of N_{TAIL}. Addition of a 2-fold molar excess of XD to spin-labeled S488C, L496C, and V517C N_{TAIL} proteins triggers a significant reduction in the radical mobility (Figure 6), thus indicating that the interaction affects the environment in proximity to these positions. These data are in agreement with previous spectroscopic studies supporting the involvement of both Box2 and Box3 in binding to XD (Figure 1A), with Box2 undergoing α-helical folding upon complex formation.[30,31] The variation in the radical mobility bound at position 517 upon addition of XD can result either from a direct interaction with the partner, although not accompanied by a gain of regular secondary structure or by a local modification induced by the proximity of XD bound to Box2. The former hypothesis is consistent with data from Bourhis et al. showing that Box3 interacts with XD.[31]

Notably, after addition of a 2-fold molar excess of XD, the reduction in the mobility of the spin label introduced at positions 488 and 496 is more pronounced than that observed for the radical at position 517 (Figure 6). These data support either a higher inherent flexibility of Box3 as compared to Box2, a higher gain of rigidity of Box2 induced by XD as compared to Box3, or a combination of both effects. That Box2 gains a higher rigidity is consistent with previous spectroscopic studies indicating that Box2 undergoes more dramatic structural changes upon binding to XD as compared to Box3.[31] Thus, SDSL EPR spectroscopy provides quantitative insights into the conformational changes that the IDP undergoes in the presence of a partner, possibly reflecting binding versus binding-coupled-to-folding events.

However, no reduction in the radical mobility was observed upon interaction of XD with spin-labeled S407C (Figure 6). This lack of reduction in the radical mobility is accounted for by the lack of involvement of Box1 in the interaction with XD, in agreement with previously reported spectroscopic studies, ruling out a role for Box1 in binding to XD (Figure 1A).[31]

Although TFE induces a significant drop in the mobility of spin labels at positions 488 and 496, this variation is much less pronounced than that observed in the presence of XD. These differences between TFE and XD can likely be ascribed either to the ability of XD to stabilize the formation of the α-MoRE (with this latter being only transiently populated by the unbound form of N_{TAIL} in the presence of TFE) or to a restrained motion of the backbone due to the presence of XD.

Equilibrium displacement experiments not only show the reversibility of the N_{TAIL}−XD interaction but also indicate the reversibility of the induced folding of the α-MoRE upon the dissociation of XD. Indeed, our results indicate that upon dissociation of XD the spin-labeled S488C and L496C proteins exhibit a spectral signature corresponding to the free form, consistent with a loss of α-helicity. These results represent the first experimental evidence indicating that N_{TAIL} adopts its original premolten globule conformation after the dissociation of its partner.

Our results also point out that the unlabeled S407C N_{TAIL} protein displays the same ability to shift the equilibrium toward the unbound form as that of the wt N_{TAIL} protein, suggesting that S407C and wt N_{TAIL} proteins exhibit a similar affinity toward XD. However, we could not measure the apparent K_D values of all the spin-labeled proteins, because in the range of 0−50% of N_{TAIL}−XD complex, the observed variations in the $h(+1)/h(0)$ ratio were within the error bar (Figure 2D and data not shown). Nevertheless, CD analyses ruled out the possibility that both mutagenesis and spin-labeling may have affected the overall secondary structure content of N_{TAIL} as well as its propensity to fold (Figure 3).

In the presence of 30% sucrose, i.e., under conditions in which the intrinsic motion of the protein becomes negligible with respect to the intrinsic motion of the spin label, the EPR line shape of both spin-labeled S488C and L496C bound to XD is similar to that observed by Mchaourab et al. for nitroxide side chains located at the solvent-accessible surfaces of α-helices in T4 lysozyme.[38] Furthermore, a slightly higher drop in the mobility of the spin label is observed for L496C as compared to S488C. We can speculate that this difference may reflect a more constrained motion of the spin label at position 496 as compared to that at position 488, because of their different locations relative to the α-MoRE. Indeed, while the spin label grafted at position 488 is located at the beginning of the α-MoRE, that grafted at position 496 is situated in the middle. That the extremities of α-helices are more mobile than their central parts has already been well-documented by SDSL EPR spectroscopy.[38] However, the addition of XD triggers only a modest reduction in the mobility of the spin label grafted at position 517 with respect to the shifts observed for both spin-labeled S488C and L496C proteins. This observation is consistent with previous data indicating that Box3 does not undergo α-helical folding upon binding to XD.[31] In further support of the lack of α-helical folding of Box3, the EPR spectrum of the V517C−XD complex does not exhibit the typical signature that is observed in the spectra of the S488C−XD and L496C−XD complexes that is attributable to an α-helix.

Comparison between SDSL EPR Spectroscopy and Other Spectroscopic Techniques. The results herein described point

out the suitability of SDSL EPR spectroscopy in assessing induced folding events of IDPs. Protein regions involved in structural transitions could be readily identified, thus providing information at the residue level. As compared to NMR, which is the most powerful technique to document regular (α or β) structural transitions, SDSL EPR spectroscopy has the advantage of being less demanding in terms of protein amounts (nanomoles versus micromoles). Moreover, while NMR backbone assignment for large proteins is still challenging, SDSL EPR spectroscopy can be used with various proteins independently of their molecular masses. CD is another convenient method enabling the assessment of the gain of regular secondary structure of IDPs upon binding to a partner/ligand. However, this technique suffers from the drawback of providing information about the *overall* secondary structure content but no information about the distinct contributions of various protein regions (see refs 29 and 31). Conversely, SDSL EPR spectroscopy provides such information because it detects structural variations in the environment close to the radical. Thus, information about the folding propensities of specific protein regions can be obtained just through site-directed mutagenesis, a protein modification in principle less dramatic than a deletion. One has to check however that mutagenesis and spin-labeling do not affect the biochemical properties of the protein. It is noteworthy that this approach should turn out to be particularly successful for IDPs, as they are generally more tolerant to point mutations as compared to globular proteins, because of the lack of a rigid scaffold and of the sequence hypervariability that typifies them.[63] That biophysical approaches based on cysteine site-directed mutagenesis can be successfully used for the study of IDPs is well illustrated by the work of Hauer et al., who characterized the induced folding of the inhibitor of the cAMP-dependent protein kinase upon binding to the catalytic subunit of the latter using fluorescence anisotropy.[64]

Conclusions

In this paper we used SDSL EPR spectroscopy to assess the induced folding, i.e., the disorder-to-order transition, of the intrinsically disordered C-terminal N_{TAIL} domain of the measles virus nucleoprotein in the presence of either the secondary structure stabilizer TFE or one of its physiological partners, namely, the C-terminal domain of the viral phosphoprotein, XD. We show that (1) different N_{TAIL} regions contribute to a different extent to the induced folding process, (2) XD promotes a structural transition in the proximity of positions 488 and 496 that is indicative of an α-helical transition, (3) the induced folding event is a reversible phenomenon, (4) the N-terminus of N_{TAIL} has a previously undetected structural propensity that may be relevant in terms of induced folding of N_{TAIL} upon binding to another, extracellular partner, and (5) the C-terminus of N_{TAIL} "resists" gaining structure even at TFE concentrations as high as 40%, thereby highlighting the relevance of studies making use of TFE to infer information about structural propensities of proteins.

This work constitutes the first report of the induced folding of an IDP assessed by SDSL EPR spectroscopy. It validates this approach for monitoring structural transitions of IDPs in the presence of their partner(s), thus paving the way toward the characterization of other IDPs. Moreover, this work extends our previous data on the $N_{TAIL}-XD$ interaction, thus contributing to the field of protein−protein interactions and, in particular, to the rapidly growing field of IDPs.

Acknowledgment. We are very grateful to Bruno Canard for his constant support and encouragement. We also thank Véronique Receveur-Bréchot for a critical reading of the manuscript and for useful discussions and Sébastien Ranaldi and Ahmad Allouch for help in recording the EPR spectra. This work was supported by the CNRS and was partly carried out with financial support from the Agence Nationale de la Recherche, Specific Program "Microbiologie et Immunologie", ANR-05-MIIM-035-02, "Structure and Disorder of Measles Virus Nucleoprotein: Molecular Partnership and Functional Impact".

References and Notes

(1) Dunker, A. K.; Lawson, J. D.; Brown, C. J.; Williams, R. M.; Romero, P.; Oh, J. S.; Oldfield, C. J.; Campen, A. M.; Ratliff, C. M.; Hipps, K. W.; Ausio, J.; Nissen, M. S.; Reeves, R.; Kang, C.; Kissinger, C. R.; Bailey, R. W.; Griswold, M. D.; Chiu, W.; Garner, E. C.; Obradovic, Z. *J. Mol. Graphics Modell.* **2001**, *19*, 26.

(2) Tompa, P. *Trends Biochem. Sci.* **2002**, *27*, 527.

(3) Uversky, V. N. *Protein Sci.* **2002**, *11*, 739.

(4) Tompa, P. *J. Mol. Struct. (THEOCHEM)* **2003**, *666*−*67*, 361.

(5) Fink, A. L. *Curr Opin Struct Biol* **2005**, *15*, 35.

(6) Dyson, H. J.; Wright, P. E. *Nat. Rev. Mol. Cell Biol.* **2005**, *6*, 197.

(7) Uversky, V. N.; Oldfield, C. J.; Dunker, A. K. *J. Mol. Recognit.* **2005**, *18*, 343.

(8) Dunker, A. K.; Obradovic, Z. *Nat. Biotechnol.* **2001**, *19*, 805.

(9) Fuxreiter, M.; Simon, I.; Friedrich, P.; Tompa, P. *J. Mol. Biol.* **2004**, *338*, 1015.

(10) Bienkiewicz, E. A.; Adkins, J. N.; Lumb, K. J. *Biochemistry* **2002**, *41*, 752.

(11) Lacy, E. R.; Filippov, I.; Lewis, W. S.; Otieno, S.; Xiao, L.; Weiss, S.; Hengst, L.; Kriwacki, R. W. *Nat. Struct. Mol. Biol.* **2004**, *11*, 358.

(12) Lamb, R. A.; Kolakofsky, D. In *Fields Virology*, 4th ed.; Fields, B. N., Knipe, D. M., Howley, P. M., Eds.; Lippincott-Raven: Philadelphia, PA, 2001; pp 1305−1340.

(13) Karlin, D.; Longhi, S.; Canard, B. *Virology* **2002**, *302*, 420.

(14) Kingston, R. L.; Walter, A. B.; Gay, L. S. *J. Virol.* **2004**, *78*, 8615.

(15) Longhi, S.; Receveur-Brechot, V.; Karlin, D.; Johansson, K.; Darbon, H.; Bhella, D.; Yeo, R.; Finet, S.; Canard, B. *J. Biol. Chem.* **2003**, *278*, 18638.

(16) Heggeness, M. H.; Scheid, A.; Choppin, P. W. *Proc. Natl. Acad. Sci. U.S.A.* **1980**, *77*, 2631.

(17) Heggeness, M. H.; Scheid, A.; Choppin, P. W. *Virology* **1981**, *114*, 555.

(18) tenOever, B. R.; Servant, M. J.; Grandvaux, N.; Lin, R.; Hiscott, J. *J. Virol.* **2002**, *76*, 3659.

(19) Zhang, X.; Glendening, C.; Linke, H.; Parks, C. L.; Brooks, C.; Udem, S. A.; Oglesbee, M. *J. Virol.* **2002**, *76*, 8737.

(20) Zhang, X.; Bourhis, J. M.; Longhi, S.; Carsillo, T.; Buccellato, M.; Morin, B.; Canard, B.; Oglesbee, M. *Virology* **2005**, *337*, 162.

(21) De, B. P.; Banerjee, A. K. *Microsc. Res. Tech.* **1999**, *47*, 114.

(22) Moyer, S. A.; Baker, S. C.; Horikami, S. M. *J. Gen. Virol.* **1990**, *71*, 775.

(23) Laine, D.; Trescol-Biémont, M.; Longhi, S.; Libeau, G.; Marie, J.; Vidalain, P.; Azocar, O.; Diallo, A.; Canard, B.; Rabourdin-Combe, C.; Valentin, H. *J. Virol.* **2003**, *77*, 11332.

(24) Laine, D.; Bourhis, J.; Longhi, S.; Flacher, M.; Cassard, L.; Canard, B.; Sautès-Fridman, C.; Rabourdin-Combe, C.; Valentin, H. *J. Gen. Virol.* **2005**, *86*, 1771.

(25) Karlin, D.; Longhi, S.; Receveur, V.; Canard, B. *Virology* **2002**, *296*, 251.

(26) Karlin, D.; Ferron, F.; Canard, B.; Longhi, S. *J. Gen. Virol.* **2003**, *84*, 3239.

(27) Johansson, K.; Bourhis, J. M.; Campanacci, V.; Cambillau, C.; Canard, B.; Longhi, S. *J. Biol. Chem.* **2003**, *278*, 44567.

(28) Oldfield, C. J.; Cheng, Y.; Cortese, M. S.; Romero, P.; Uversky, V. N.; Dunker, A. K. *Biochemistry* **2005**, *44*, 12454.

(29) Bourhis, J.; Johansson, K.; Receveur-Bréchot, V.; Oldfield, C. J.; Dunker, A. K.; Canard, B.; Longhi, S. *Virus Res.* **2004**, *99*, 157.

(30) Kingston, R. L.; Hamel, D. J.; Gay, L. S.; Dahlquist, F. W.; Matthews, B. W. *Proc. Natl. Acad. Sci. U.S.A.* **2004**, *101*, 8301.

(31) Bourhis, J. M.; Receveur-Bréchot, V.; Oglesbee, M.; Zhang, X.; Buccellato, M.; Darbon, H.; Canard, B.; Finet, S.; Longhi, S. *Protein Sci.* **2005**, *14*, 1975.

(32) Bourhis, J. M.; Canard, B.; Longhi, S. *Virologie* **2005**, *9*, 367.

(33) Bourhis, J. M.; Canard, B.; Longhi, S. *Virology* **2006**, *344*, 94.

(34) Feix, J. B.; Klug, C. S. Site-directed spin-labeling of membrane proteins and peptide−membrane interactions. In *Spin Labeling: The Next Millenium*; Berliner, L., Ed.; Biological Magnetic Resonance 14; Plenum Press: New York, 1998; p 251.

(35) Hubbell, W. L.; Gross, A.; Langen, R.; Lietzow, M. A. *Curr. Opin. Struct. Biol.* **1998**, *8*, 649.

(36) Biswas, R.; Kuhne, H.; Brudvig, G. W.; Gopalan, V. *Sci. Prog.* **2001**, *84*, 45.
(37) Hubbell, W. L.; Altenbach, C.; Hubbell, C. M.; Khorana, H. G. *Adv. Protein Chem.* **2003**, *63*, 243.
(38) Mchaourab, H. S.; Lietzow, M. A.; Hideg, K.; Hubbell, W. L. *Biochemistry* **1996**, *35*, 7692.
(39) Popp, S.; Packschies, L.; Radzwill, N.; Vogel, K. P.; Steinhoff, H. J.; Reinstein, J. *J. Mol. Biol.* **2005**, *347*, 1039.
(40) Kreimer, D. I.; Szosenfogel, R.; Goldfarb, D.; Silman, I.; Weiner, L. *Proc. Natl. Acad. Sci. U.S.A.* **1994**, *91*, 12145.
(41) Qu, K.; Vaughn, J. L.; Sienkiewicz, A.; Scholes, C. P.; Fetrow, J. S. *Biochemistry* **1997**, *36*, 2884.
(42) Kriwacki, R. W.; Hengst, L.; Tennant, L.; Reed, S. I.; Wright, P. E. *Proc. Natl. Acad. Sci. U.S.A.* **1996**, *93*, 11504.
(43) Uversky, V. N. *Eur. J. Biochem.* **2002**, *269*, 2.
(44) Dyson, H. J.; Wright, P. E. *Curr. Opin. Struct. Biol.* **2002**, *12*, 54.
(45) Uversky, V. N.; Oldfield, C. J.; Dunker, A. K. *J. Mol. Recognit.* **2005**, *18*, 343.
(46) Dunker, A. K.; Cortese, M. S.; Romero, P.; Iakoucheva, L. M.; Uversky, V. N. *FEBS J.* **2005**, *272*, 5129.
(47) Fletcher, C. M.; McGuire, A. M.; Gingras, A. C.; Li, H.; Matsuo, H.; Sonenberg, N.; Wagner, G. *Biochemistry* **1998**, *37*, 9.
(48) Receveur-Bréchot, V.; Bourhis, J. M.; Uversky, V. N.; Canard, B.; Longhi, S. *Proteins: Struct., Funct., Bioinf.* **2006**, *62*, 24.
(49) Uversky, V. N. *Biochemistry* **1993**, *32*, 13288.
(50) Guigliarelli, B.; Asso, M.; More, C.; Augier, V.; Blasco, F.; Pommier, J.; Giordano, G.; Bertrand, P. *Eur. J. Biochem.* **1992**, *207*, 61.
(51) Goldman, A.; Bruno, G. V.; Polnaszek, C. F.; J. H., F. *J. Chem. Phys.* **1972**, *56*, 716.
(52) Marsh, D.; Kurad, D.; Livshits, V. A. *Chem. Phys. Lipids* **2002**, *116*, 93.
(53) Morris, M. C.; Mery, J.; Heitz, A.; Heitz, F.; Divita, G. *J. Pept. Sci.* **1999**, *5*, 263.
(54) Diallo, A.; Barrett, T.; Barbron, M.; Meyer, G.; Lefevre, P. C. *J. Gen. Virol.* **1994**, *75*, 233.
(55) Iakoucheva, L.; Kimzey, A.; Masselon, C.; Smith, R.; Dunker, A.; Ackerman, E. *Protein Sci.* **2001**, *10*, 1353.
(56) Hua, Q. X.; Jia, W. H.; Bullock, B. P.; Habener, J. F.; Weiss, M. A. *Biochemistry* **1998**, *37*, 5858.
(57) Knowles, P. F.; Marsh, D.; Rattle, H. W. E. *Magnetic Resonance of Biomolecules*; John Wiley & Sons Ltd: New York, 1976.
(58) Sivakolundu, S. G.; Bashford, D.; Kriwacki, R. W. *J. Mol. Biol.* **2005**, *353*, 1118.
(59) Luo, Y.; Baldwin, R. L. *J. Mol. Biol.* **1998**, *279*, 49.
(60) Buck, M.; Schwalbe, H.; Dobson, C. M. *Biochemistry* **1995**, *34*, 13219.
(61) Fan, P.; Bracken, C.; Baum, J. *Biochemistry* **1993**, *32*, 1573.
(62) Fasman, G. D. *Circular Dichroism and Conformational Analysis of Biomolecules*; Plenum Press: New York, 1996.
(63) Brown, C. J.; Takayama, S.; Campen, A. M.; Vise, P.; Marshall, T. W.; Oldfield, C. J.; Williams, C. J.; Dunker, A. K. *J. Mol. Evol.* **2002**, *55*, 104.
(64) Hauer, J. A.; Taylor, S. S.; Johnson, D. A. *Biochemistry* **1999**, *38*, 6774.